

# Demonstration of a Signal Enhanced Fast Raman Sensor for Human Breath Analysis

Sebastian Schlüter, Thomas Seeger

Institute of Engineering Thermodynamics, University of  
Siegen, 57076, Siegen, Germany  
thomas.seeger@uni-siegen.de

Gennadij Lukyanov

Saint Petersburg National Research University of  
Information Technologies, Mechanics and Optics, Saint  
Petersburg, Russia  
gen-lukjanow@yandex.ru

**Abstract**—A gas sensor based on spontaneous Raman scattering is proposed for the compositional analysis of single breath events and for an anesthesia simulation under clinical relevant conditions. A description of the sensor as well as a comprehensive characterization of the system is carried out in order to determine the measurement uncertainty. Finally, the sensor is applied to consecutive breath events and allowed measurements with 250 ms time resolution. The Raman sensor is able to detect all the major gas components, i.e. N<sub>2</sub>, O<sub>2</sub>, CO<sub>2</sub>, and H<sub>2</sub>O at ambient pressure with a high temporal resolution. Also the volatile anesthetic agents N<sub>2</sub>O, sevoflurane, desflurane and isoflurane were detected during a simulated anesthesia procedure. Concentration fluctuations within a single breath event could be resolved.

## I. INTRODUCTION

An on-line species concentration determination of gas mixtures is of great interest in a wide range of technical and medical applications. For process reasons the gas sample has often a relatively low pressure of some 100 hPa. Typical examples for such gas mixtures are biogas or natural gas [1–3]. Their gas composition and gas properties like the caloric value and the density is strongly depending on the production process or the exploration site. This has to be taken into account when the gas is injected into the existing gas supply net or used in a combustion process. In either case, the final product gas composition has to be monitored. Another example is the human breath analysis in form of breathing gas analysis of a patient in general or during an anesthesia procedure.

The breathing gas analysis is of interest in the so-called respiratory function studies [4], which will be used to estimate the state of the respiratory tract. There are studies based on measurements [5–7] and simulation [8], [9] of dynamic processes during respiration. In recent years there has been a steady tendency to focus these studies on the gas composition of exhaled air [10–12]. Therefore is more and more important to develop new methods and technologies which have the potential for an online sensor system that allows a precise measurement of the gas composition of the exhaled air. In this case also a fast data acquisition of all gas species within a time resolution of 200 ms to 500 ms is necessary in order to clearly resolve the dynamic behavior of each breath event. This requirement can be fulfilled by spectroscopic techniques.

On the other hand the continuous monitoring of this gas composition is of vital importance to ensure the patients safety. Therefore the concentration of the various anesthetic gases, which are added to the breathing gas and the oxygen, carbon dioxide and water vapor concentration, is necessary to be monitored [13]. Since inspired and expired breathing cycles take place within a few seconds the gas composition is changing rapidly. Also this application requires a fast and precise measurement of all gas species within a time resolution of 200 ms to 500 ms during each breath event [14].

Therefore we demonstrate the potential of the spontaneous Raman technique for these applications. The presented sensor requires no sample preparation and can detect O<sub>2</sub>, CO<sub>2</sub>, N<sub>2</sub> and H<sub>2</sub>O and all four anesthetic agents, at a pressure of 980 hPa. Further, the system can be extended via software update to new gas components. In this paper such sensor system based on spontaneous Raman scattering for fast and accurate gas analysis during an anesthesia procedure is presented.

## II. MEASUREMENT PRINCIPLE

The well-known principles of spontaneous Raman scattering can be found in literature (see e.g. [15], [16]). Therefore only a brief summary is presented here. When an electromagnetic wave (i.e. laser beam) with the energy  $E = h\nu_0$  passes through a gas volume that is containing molecules (no noble gases) several scattering processes may occur. Depending on the energy  $E$  of the electromagnetic wave, on the molecule density  $n$ , species and temperature one can observe elastic scattering processes, such as Rayleigh scattering. One order of magnitude smaller, inelastic scattering appears, modifying the rotational and vibrational energy of the molecules, which are exposed to the incoming light. Due to energy conservation the frequency  $\nu_{S/AS}$  of the scattered light is shifted referring to the frequency  $\nu_0$  of the incident laser light. The frequency-shifted radiation is termed as Raman scattering. Depending on whether the involved molecule absorbs or emits energy a distinction in two cases is possible between the red shifted Stokes Raman scattering ( $\nu_S = \nu_0 - \Delta\nu_R$ ) and the blue shifted anti-Stokes Raman scattering ( $\nu_{AS} = \nu_0 + \Delta\nu_R$ ). The size of the frequency shift results from the difference in the rotational and vibrational energy levels of the molecule involved:

$$\Delta\nu_R = T'(v', J') - T''(v'', J'') \quad (1)$$

Single prime marked parameters indicate the upper energy level, and the parameters marked with two primes indicate the lower energy state of the molecule. The energy term  $T(v, J)$  consist of the energy values of the vibration and rotation of the molecule and is related to the vibrational quantum number  $J$ . For instance in case of diatomic molecules like  $N_2$ , the energy term can be expressed by:

$$\begin{aligned} T(v, J) = & w_e \left( v + \frac{1}{2} \right) - w_e x_e \left( v + \frac{1}{2} \right)^2 + \\ & \dots + \left[ B_e - a_e \left( v + \frac{1}{2} \right) + \dots \right] J(J+1) - \\ & \dots - \left[ D_e + b_e \left( v + \frac{1}{2} \right) + \dots \right] J^2(J+1)^2 + \dots \end{aligned} \quad (2)$$

Here,  $\omega_e$ ,  $\omega_e x_e$ ,  $B_e$ ,  $a_e$ ,  $D_e$  and  $\beta_e$  are molecule specific constants which can be found in compilation data books [17, 18] for diatomic and polyatomic molecules. From equation (2) one can see that the energy is only influenced by molecule specific constants. Consequently, also the Raman shift is a molecule specific parameter and can be used as a fingerprint for the explicit determination of this particular molecule [19].

In a gas mixture of species which interact to a moderate degree, the Raman spectrum will generally be a superposition of the Raman spectra of the components within the mixture [16, 20]. Since each molecule has its unique frequency spectrum for an individual species the frequency shift of the Raman signal  $\Delta\omega_R$ , can either be used for species identification or, by measuring the signal intensity, for a quantitative analysis of gas samples [21, 22]. The detected intensity  $I_i$  of a vibrational Stokes Raman line of species  $i$  can be written as [23].

$$I_i = k\Omega \frac{\partial\sigma}{\partial\Omega} n_i I_0 \quad (3)$$

Where  $\Omega$  is the collecting solid angle,  $\partial\sigma/\partial\Omega$  is the differential scattering cross section depending on molecular-specific parameters such as isotropy and anisotropy of the polarizability tensor  $\alpha$  and also depending on the geometry of the setup. The parameter  $l$  is the length of the probe volume and  $I_0$  is the incident laser intensity. The factor  $k$  depends on the experimental setup, and takes into account the geometry and wavelength dependent losses,  $n_i$  is the parameter of interest for concentration measurements, i.e. the number density of the specific gas species  $i$  inside the probe volume [16, 19]. In order to overcome the problem of laser intensity fluctuations, which would linearly influence the evaluated number density to be determined, it is common approaches to evaluate relative species concentrations by determine the signal intensity ratio of two species from a spectrum. This can be written as [20]:

$$\frac{I_i}{I_j} = \frac{k\Omega \left( \frac{\partial\sigma}{\partial\Omega} \right)_i n_i I_0}{k\Omega \left( \frac{\partial\sigma}{\partial\Omega} \right)_j n_j I_0} = C \frac{n_i}{n_j} \quad (4)$$

### III. SENSOR SETUP

The sensor system includes a cw Nd:YVO<sub>4</sub> laser which operates at  $\lambda = 532$  nm. The Raman signals are measured by a spectrometer in combination with a back-thinned CCD chip. The laser beam is focused into a test cell. The Raman scattered light is collected perpendicular to the incident laser beam by a telescope with a large solid angle on the collecting side and an optical filter to suppress the unwanted Rayleigh signal. Spatial resolution is not of interest here. The light is then focused into an optical fiber with 200  $\mu\text{m}$  core diameter and guided to a spectrometer with a back-thinned CCD area sensor with a peak quantum efficiency of 90 %. Thermal noise is minimized by thermal conditioning of the CCD detector. The detectable spectral range is from 530 nm to 620 nm resulting in a Raman shift from 0  $\text{cm}^{-1}$  to 2700  $\text{cm}^{-1}$ . Raman spectra of interest, as shown in Fig. 1, are the volatile anesthetics like sevoflurane (SEV), desflurane (DES), isoflurane,  $N_2O$  and respiratory gases  $N_2$ ,  $O_2$ ,  $CO_2$  and  $H_2O$ .

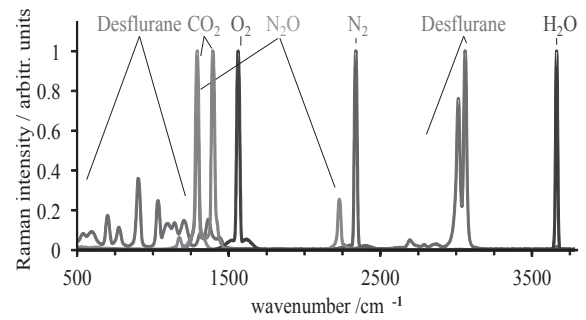


Fig. 1. Gas phase Raman spectra of species typical for anesthetic breathing

Due to the relatively low Raman signal intensity, it is challenging to realize short measurement times for low-pressure gas samples. In order to increase the Raman signal intensities significantly and as a result to achieve short measurement times, a multipass approach was used. The basic amplification principle in all these types of cavities always is the same. The stimulating laser beam passes through the measurement volume as often as possible. Starting from a robust 90°-setup, two suitable multipass arrangements are compared here (Fig. 2) regarding their signal amplification in order to find the most suitable one. The signal gain of such a multipass arrangement is dominated by the optical losses per pass. The reflectivity and transmissivity of the individual surfaces in the beam pass have a huge impact to the single-pass efficiency  $\eta$  which is defined as

$$\eta = \left( \prod_{i=0}^{m-1} R_i \right) \left( \prod_{j=0}^{k-1} T_j \right) \quad (5)$$

where the number of reflective surfaces is given by  $i$  and the number of translucent components by  $j$ ,  $R_i$  describes the reflectivity of the surface  $i$  and  $T_j$  the transmissivity of surface  $j$ . If all  $R_i$  and  $T_j$  have equal values, equation (5) can be simplified to

$$\eta = R^{m-1} T^{k-1} \quad (6)$$

The signal gain is given by

$$G_A = \frac{1 - \eta^p}{1 - \eta} \quad (7)$$

where  $p$  is the number of passes. The limit for  $p \rightarrow \infty$  shows the maximum achievable gain for a given cavity efficiency  $\eta$ .

$$\lim_{p \rightarrow \infty} G_A = \frac{1}{1 - \eta} \quad (8)$$

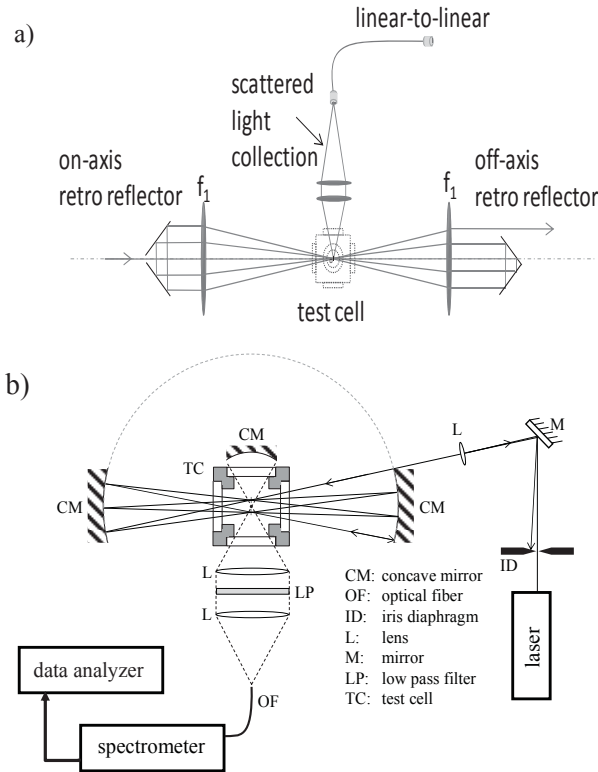


Fig. 2. Retro-reflecting cavity (RRC) with plane mirrors and focusing lenses (a) and near-confocal cavity (NCC) with confocal mirrors (b)

In Fig. 3 the measured signal gain of the near-confocal cavity (NCC) and the retro-reflecting cavity (RRC) are compared to find the most suitable for the sensor system. The signal gain for  $O_2$ ,  $N_2$  and  $H_2O$  were determined, since they are well distributed over the spectral region of interest. In the case of the RRC, only six passes could be realized in the experiment. As it can be seen from Fig. 2a the RRC-type has a diverging beam propagation. After each pass the distance between the central axis of the cavity and exciting beam increases, therefore lens aberration also increases with the number of passes. In the case of the NCC-type 52 beam passes could be realized. The limiting factors in the case of the NCC-type were the size of the concave mirrors and the beam acceptance angle of the sample cell. From these measurements, the respective  $\eta$  can be determined and compared as shown in Fig. 3. Subsequently the maximal possible gain amplification can be calculated from equation (5), which results in a theoretical maximum signal gain of  $G_{Max,NCC} = 18.52$  and  $G_{Max,RRC} = 10$ . The NCC needs

compared to the RRC less optical components. Therefore, a relatively large  $\eta_{NCC}$  can be achieved. Beside that, depending on the size of the mirrors, a large number of passes can be realized in the NCC-type which ultimately leads to larger signal amplification. One problem with the NCC-type is that the laser beam is back-reflected exactly to its origin when the maximum number of passes is realized. In the experiment, the cavity adjustment was slightly misaligned, so that the outgoing beam was deflected a little, to prevent it from entering the laser source again (see Fig. 2b).

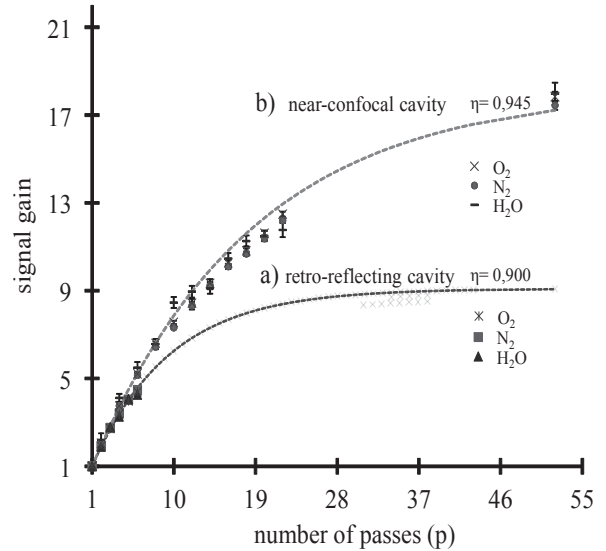


Fig. 3. Experimental comparison of the signal gain for retro-reflecting cavity (a) and near-confocal cavity (b)

Based on these results a NCC cavity was used for the sensor system. The laser beam is guided into this multipass cavity which focuses the beam into a measurement cell. The volume of this cell was approximately 20 ml. In this case 52 beam passes could be realized. The limiting factors were the size of the concave mirrors and the beam acceptance angle of the sample cell. The Raman scattered light is collected perpendicular to the incident laser beam by a telescope optic with a large solid angle on the collecting side and an optical filter to suppress unwanted stray light and the Rayleigh line. Additionally the light which is scattered at an angle of  $270^\circ$  is redirected in the collecting optics. The signal is then focused into an optical fiber and guided into a spectrometer with a back-thinned CCD sensor. Thermal noise is minimized by thermal conditioning of the CCD chip.

#### IV. EVALUATION PROCEDURE

For the evaluation of the Raman signals the setup was calibrated once using a gas mixture including all species of interest at known concentrations. Since measurements are usually done in the range of ATP-conditions („ambient temperature and pressure“) and not on a large scale may be varied, it is not necessary to take temperature or pressure dependency of the Raman cross section into account. Next, the spectra of all pure gases ( $N_2$ ,  $O_2$ ,  $N_2O$ ,  $CO_2$ , SEV, isoflurane, DES) were recorded at same conditions and stored in a

database. To determine the concentration of measured spectra a contour fit algorithm (see e.g. [24]) was applied. In this procedure a synthetic spectrum is generated from weighted spectra of the pure gas components, and compared to the measured mixture spectrum using a fitting routine. The contour fit works best if the SNR of the measured spectra has a high value and if the Raman bands are well separated. But even if they partly overlap the contour fit method provides acceptable results. Since some of the anaesthetic agents are not used in combination with each other or parallel to each other, the effect of spectral line overlapping is considerable small. For instance  $\text{N}_2\text{O}$  and  $\text{CO}_2$  overlap at  $1300\text{ cm}^{-1}$  but  $\text{N}_2\text{O}$  provides another peak at  $2230\text{ cm}^{-1}$  and also  $\text{CO}_2$  one at  $1390\text{ cm}^{-1}$ . This peaks are well isolated and don't interfere with other bands. Therefore they can be well used for a concentration determination.

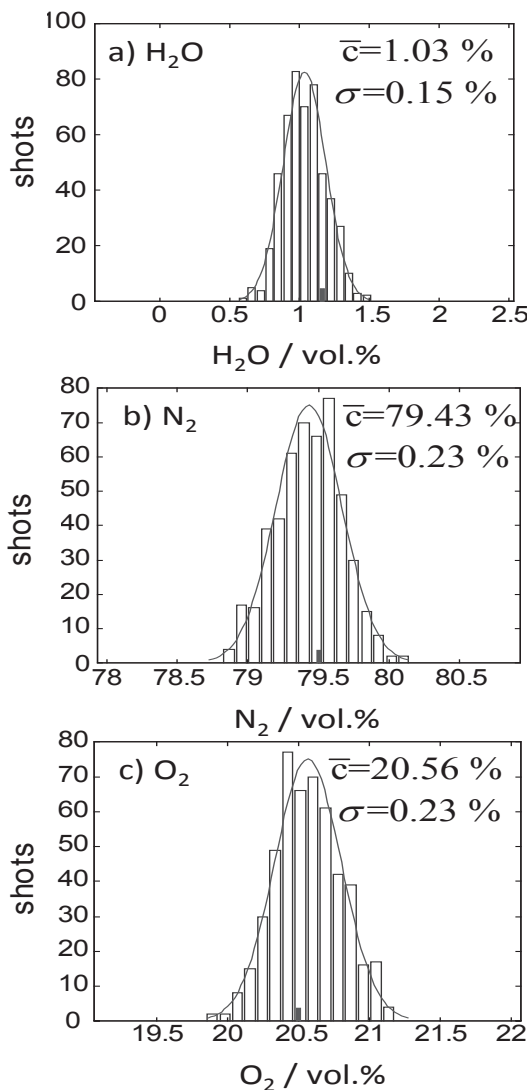


Fig. 4. Histogram of 500 single shot Raman measurements

The precision and accuracy of the Raman system was tested by monitoring and evaluating 500 single shot Raman spectra taken in room air and synthetic air at 981 hPa and 294 K. The time resolution was 250 ms. The  $\text{H}_2\text{O}$  concentration

distribution measured in room air is shown in Fig. 4a. A mean  $\text{H}_2\text{O}$  concentration of 1.03 vol. % and a standard deviation of 0.15 % was achieved. Corresponding hygrometer measurements show a  $\text{H}_2\text{O}$  concentration of 1.16 vol. %. The synthetic air consists of 79.5 vol. %  $\text{N}_2$  and 20.5 vol. %  $\text{O}_2$ . The corresponding Raman concentration distributions were shown in Fig. 4b and 4c together with the mean values and the standard deviations.

## V. EXPERIMENTAL RESULTS

With the developed Raman system human breath events it was possible to achieve inspiratory and expiratory breath events with a time resolution of 250 ms. Since there is a significant dependence of the Raman spectra on temperature and pressure, the setup was equipped with a pressure indicator and a type K thermocouple. However noticeable would be observed with this sensor system if the temperature of the sample varies more than 10 K or the pressure varies more than 1 MPa [25, 26]. This is not the case for the experiments presented in this study since the temperature variation is kept in a range of  $\pm 5\text{ K}$  and a pressure variation occurs only in a range of  $\pm 25\text{ hPa}$ .

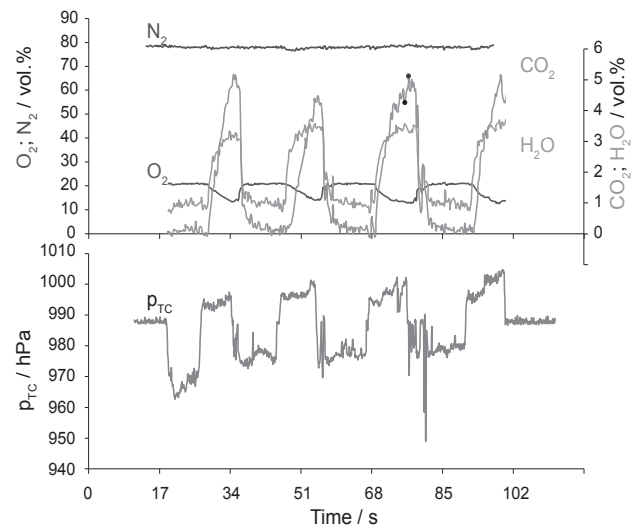


Fig. 5. Measurement series showing the species concentration and the pressure variation during three consecutive breath events

In Fig. 5 a measurement series showing three consecutive breath events is presented. At start of the measurement series typical room air with a concentration of  $\text{N}_2=78.5\text{ vol.}\%$ ,  $\text{O}_2=20.7\text{ vol.}\%$ ,  $\text{CO}_2=0.1\text{ vol.}\%$  and  $\text{H}_2\text{O}=0.69\text{ vol.}\%$  was analyzed. 17 s later a pressure drop down to 965 hPa can be observed due to the start of an inspiration. The species concentration is staying constant until the expiratory gas enters the measurement cell. At 26 s after start of the measurements the pressure is increasing up to 999 hPa caused by the start of expiration. With a time delay of 2 seconds the expiratory gas enters the measurement cell and concentration changes can be observed. Since the expiratory air has a high water vapor content ( $\text{H}_2\text{O}=3.31\text{ vol.}\%$ ), concentrations of 77.92 vol.% for  $\text{N}_2$ , 13.60 vol.% for  $\text{O}_2$  and 5.18 vol.% for  $\text{CO}_2$  have been

measured. All expiratory events show small concentration fluctuations. These fluctuations can clearly be resolved by the Raman sensor.

The simulation of the anesthesia procedure was performed in an anesthesia test center at the University Hospital of Erlangen. In this case the Raman sensor was operated in line to a commercial anesthetic gas monitor (AGM, Dräger Perseus®). The anesthesia machine consists of a gas mixer, a circular system with CO<sub>2</sub> absorber and a ventilator; it delivers breathing and anesthetic gases. Calibration measurements were performed for N<sub>2</sub>, O<sub>2</sub>, N<sub>2</sub>O and CO<sub>2</sub> by using a commercial available calibration gas. The system was connected to a human pain simulator® (HPS) which has a realistic breathing behavior and delivers depending on the surgery status a clinical relevant respiratory gas composition for the expiratory gases. The online Raman measurements were performed with a continuous gas flow through the test cell. The operation of the Raman sensor needed no sample preparation and was connected directly to the y-piece of the semi-closed anesthetic circle system. Nevertheless for the conventional monitoring system the sample gas had to be dried and was therefore guided through a water trap. Based on this experimental setup Raman spectra of respiratory gas mixtures consisting of O<sub>2</sub>, N<sub>2</sub>, CO<sub>2</sub>, H<sub>2</sub>O, SEV, DES and isoflurane were recorded with the Raman sensor under clinical relevant conditions. The measurement and evaluation time for the Raman probe was set to 250 ms / spectrum for all measurements. The spectra were evaluated online and compared to measurement results achieved by the AGM.

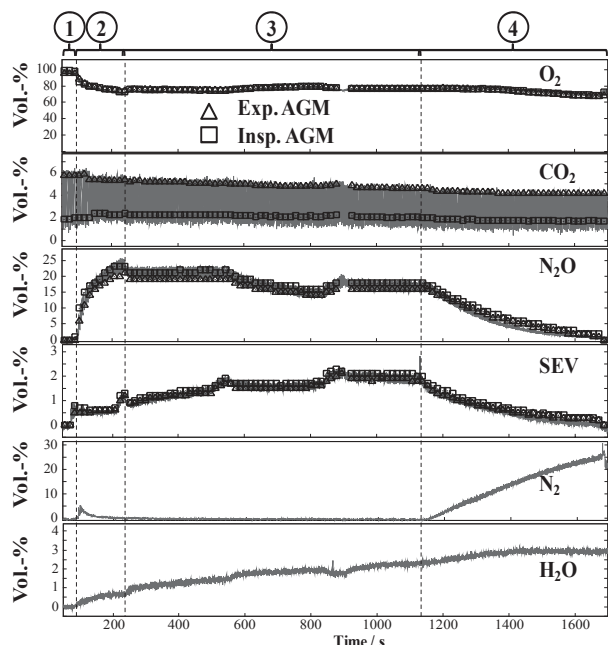
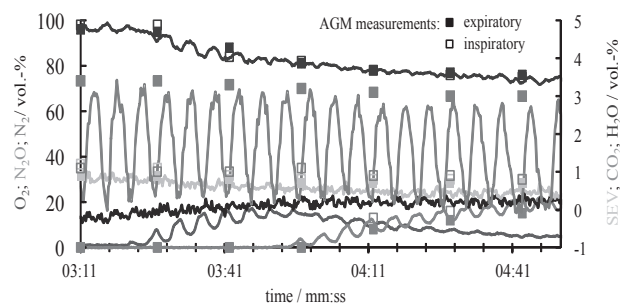


Fig. 6. Comparison of the Raman-Probe and an AGM. Anesthesia phases: 1: preoxygenation phase, 2: lead-in phase, 3: anesthesia, 4: drain-out phase

As an example, a measurement series taken over 25 minutes is shown in Fig. 6. In this example SEV was used as anesthetic agent. Due to software limitations by the AGM, each 16 sec one complete dataset containing the inspiratory and expiratory

concentration was displayed and stored. A comparison for both sensor systems based on these data is shown in Fig. 6. The illustrated time period shows a preoxygenation phase (1) to increase the arterial oxygen level of the patient for safety reasons. During the induction phase (2) the concentration of SEV increases to 2 vol.-% and nitrous oxide has a concentration of about 32 vol.-%, the O<sub>2</sub> level therefore decreases down to 65 vol.-%. To maintain the anesthesia in phase (3) the inspiratory SEV concentration is between 1 vol.-% and 2 vol.-% and the inspiratory nitrous oxide concentration is between 30 vol.-% and 36 vol.-%. Additionally an increasing H<sub>2</sub>O concentration can be observed in phase (3) caused by water which is accumulated in the CO<sub>2</sub>-absorber (see Fig. 6). Due to an exothermic reaction the wet lime cartridges in the CO<sub>2</sub>-absorber are getting warm which leads to more humid air. In the reversal phase the concentration of the anesthetic agents decreases, SEV and nitrous oxide are drained out and replaced by N<sub>2</sub>. During the complete anesthesia procedure a very good agreement between the two monitoring systems was achieved. The Raman sensor delivered in addition the N<sub>2</sub> and the H<sub>2</sub>O concentration.

In Fig. 7 a part of the preoxygenation is shown in more detail. The species concentration measured with the Raman sensor show clearly well resolved single breathing events. The CO<sub>2</sub> concentration oscillates between 0 vol.-% and 3 vol.-%, which are typical physiological values. During the presented time interval, the O<sub>2</sub> concentration was reduced from 100 vol.-% to 80 vol.-%. Therefore the N<sub>2</sub> concentration is increasing during the first 35 sec. Then N<sub>2</sub> is subsequently replaced by N<sub>2</sub>O. The SEV and the H<sub>2</sub>O concentration is almost constant



in over this time period.

Fig. 7. A part of the preoxygenation is shown in more detail. The AGM results are represented by the empty and filled squares

With the developed Raman sensor system it is also possible to measure the different volatile anesthetic agents when they are simultaneously present in the gas sample. An example is presented in Fig. 8, which shows the concentration over time for a mixture containing seven components O<sub>2</sub>, N<sub>2</sub>, CO<sub>2</sub>, DES, SEV, N<sub>2</sub>O and H<sub>2</sub>O. The individual breath cycles are again clearly visible and the Raman signals of DES and SEV could be distinguished. In this case, the anesthesia procedure was induced with SEV, since it causes no airway irritations for the patient. Afterwards it was replaced by DES. In Fig. 8 the decreasing of SEV and the increasing of DES over 5 minutes

is perceptible. The SEV concentration, however, does not show the typical concentration fluctuations through inspiration and expiration processes, which is caused to imperfections of the HPS simulator model.

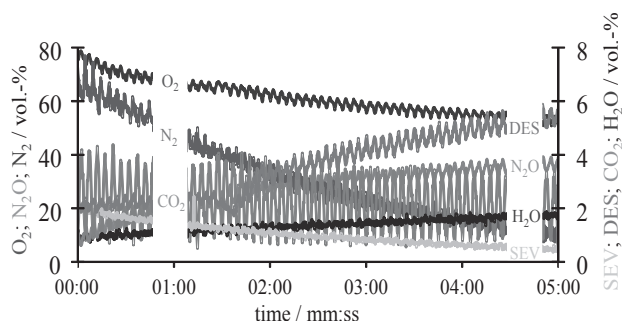


Fig. 8. Anesthesia procedure using DES and SEV

## VI. SUMMARY

In this study an online breathing gas analyzer based on linear Raman scattering was developed and tested. The Raman sensor is capable to monitor a single breath event with a time resolution of 250 ms. The Raman probe is able to measure the gas species concentration online without any sample preparation. To increase the Raman signal and to enable these short measurement times the sensor is equipped with the near-confocal cavity. All species of interest were measured online and small concentration fluctuations of 0.82 vol. % and less could clearly be resolved.

Additionally the applicability of this Raman system was used to identify and quantify all species of interest during an anesthesia procedure, which is typically at an absolute pressure of about 980 hPa performed. In contrast to established monitoring devices, the probe enables the simultaneous detection of virtually all volatile narcotic agents and respiratory relevant gases e. g. O<sub>2</sub>, CO<sub>2</sub>, N<sub>2</sub>O, SEV, isoflurane, DES and additionally N<sub>2</sub> and H<sub>2</sub>O. The Raman sensor is able to measure the gas species concentration online without any sample preparation and is thus in principal applicable as a mainstream monitor. All species of interest were monitored online and with a data acquisition time of 250 ms, which allowed to resolve a single breathing event.

## ACKNOWLEDGMENT

We would like to thank the Department of Anesthesiology, University of Erlangen-Nuremberg for their support.

## REFERENCES

- [1] J. Egermann, J. Jonuscheit, T. Seeger, A. Leipertz, "Untersuchung von diodenlaserbasierten Mehrkomponenten-Konzentrationsmesssystemen zur Gasanalyse", *Tech. Mess.*, vol. 9, 2001, pp 400-405.
- [2] S. C. Eichmann, J. Kiefer, J. Benz, T. Kempf, A. Leipertz, T. Seeger, "Determination of gas composition in a biogas plant using a Raman-based sensor system", *Meas. Sci. Technol.* vol. 25, 2014, vol. 25, 075503.
- [3] J. Kiefer, T. Seeger, S. Steuer, S. Schorsch, M. C. Weikl, A. Leipertz, "Design and characterization of a Raman-scattering-based sensor

- system for temporally resolved gas analysis and its application in a gas turbine power plant", *Meas. Sci. Technol.*, vol. 19, 2008, 085408.
- [4] A. Krotov, "Modern methodological approaches in the evaluation of nasal breathing function", *Journal of Otolaryngology*, 1998, vol. 4, pp. 51-52.
- [5] G. Lukyanov, A. Voronin, R. Neronov, "Computational modeling of airflow in nonregular shaped channels", *Scientific and Technical Journal of Information Technologies, Mechanics and Optics*, 2013, vol. 13, pp. 113-118.
- [6] G. Lukyanov, S. Polishuk, "Nonlinear dynamical modeling for interaction processes of human breathing and tachycardia on the basis of given measurements", *Scientific and Technical Journal of Information Technologies, Mechanics and Optics*, 2013, vol. 13, pp. 67-72.
- [7] G. M. Mutlu, K. W. Garey, R. A. Robbins, L. H. Danziger and I. Rubinstein, "Collection and analysis of exhaled breath condensate in humans", *American Journal of Respiratory and Critical Care Medicine*, 2001, vol. 164, pp. 731-737.
- [8] A. Voronin, G. Lukyanov, E. Frolov, "Detached-eddy simulation of turbulent airflow", *Scientific and Technical Journal of Information Technologies, Mechanics and Optics*. 2014, vol. 14, pp. 187-192.
- [9] Y. Kistenev, O. Akbasheva, O. Kutshma, "The gas composition of exhaled air and biochemical indicators of sputum in chronic obstructive pulmonary disease", *Health & Education Millennium*, 2012, vol. 14, p 68.
- [10] Y. Yanov, N. Shcherbakova, P. Nacharov, "An analysis of the gas composition of exhaled air in the diagnosis of diseases", *Russian otorhinolaryngology*, 2005, vol. 4, pp. 126-132.
- [11] J. Herbig, M. Müller, S. Schallhart, T. Titzmann, M. Graus and A. Hansel, "On-line breath analysis with PTR-TOF" *Journal of Breath Research*, 2009, vol. 3, 027004
- [12] T. Schulze-König, L. Wacker and H.-A. Sinal, "Direct radiocarbon analysis of exhaled air", *Journal of Analytical Atomic Spectrometry*, 2011, vol. 26, pp. 287-292.
- [13] Portner P. M., LaForge D. H. *Method and apparatus for pulmonary function analysis*. Patent US4083367 A (11. Apr. 1978)
- [14] American Society of Anesthesiologists, 2011, *Standards for basic anesthetic monitoring. Committee of Origin: Standards and Practice Parameters*, 2010, ASA House of Delegates ; 2010. Accessed 13 October 2014.
- [15] K. Drasner, Miller, Ronald D. Miller, *Basics of Anesthesia*, Elsevier, 2011.
- [16] A. C. Eckbreth, *Laser diagnostics for combustion temperature and species*. In: Gordon and Breach, (1996).
- [17] M. C. Tobin, "Laser Raman spectroscopy", *Chem. Anal.*, 1971, p. 11.
- [18] G. Herzberg, "Molecular spectra and molecular structure. I. Spectra of diatomic molecules", Van Nostrand, Princeton, N.J (1966).
- [19] G. Herzberg, "Molecular spectra and molecular structure. II. Infrared and Raman spectra of polyatomic molecules", Van Nostrand, Princeton, N.J. (1966).
- [20] J. Egermann, T. Seeger, A. Leipertz, "Application of 266-nm and 355-nm Nd:YAG laser radiation for the investigation of fuel-rich sooting hydrocarbon flames by Raman scattering", *Appl. Opt.* 2004, vol. 43, pp. 5564-5574.
- [21] J. Kiefer, "Dual-wavelength Raman spectroscopy approach for studying fluid-phase equilibria using a single laser", *Appl. Spectrosc.*, 2010, vol. 64, pp. 687 – 689.
- [22] J. Kiefer, T. Seeger, S. Steuer, S. Schorsch, M. C. Weikl, A. Leipertz, "Design and characterization of a Raman-scattering-based sensor system for temporally resolved gas analysis and its application in a gas turbine power plant", *Meas. Sci. & Technol.*, 2008, vol. 19, pp. 1330-1334.
- [23] S. C. Eichmann, J. Trost, T. Seeger, L. Zigan, A. Leipertz, "Application of linear Raman spectroscopy for the determination of acetone decomposition" *Opt. Exp.*, 2011, vol.19, pp. 11052-11058.
- [24] A. Leipertz, "Temperaturbestimmung in Gasen mittels linearer und nichtlinearer Raman-Prozesse", Habilitation thesis Universität Bochum, Germany, (1984).
- [25] J. Egermann, J. Jonuscheit, T. Seeger, A. Leipertz, "Investigation of diode laser-based multi-species gas sensor concepts", *Tech. Mess.*, 2001, vol. 68, pp. 400-405.
- [26] S. C. Eichmann, M. Weschta, J. Kiefer, T. Seeger, A. Leipertz, "Characterization of a fast gas analyzer based on Raman scattering for the analysis of synthesis gas" *Review of Sci. Instruments*, 2010, vol. 81, 128104.